DELIVERABLE FRONTPAGE

Project number: 243827 FP7-ENV-2009-1

Project acronym: LC-IMPACT

Project title: Development and application of environmental Life Cycle Impact assessment Methods for improved sustainability Characterisation of Technologies.

Deliverable number: D3.8

Deliverable name: Recommended assessment framework, method and characterisation factors for ecosystem impacts of acidifying emissions

Version: 1

WP number: 3

Lead beneficiary: USTUTT as WP leader, Quantis as task leader

Nature: R[1]

Dissemination level: PU[2]

Delivery date Annex I: M41

Actual delivery date: 19/03/2013

Authors: L.B. Azevedo, A. Kounina, R. van Zelm, A.J. Hendriks, M. Huijbregts, M. Margni

Comments: #

[1] Please indicate the nature of the deliverable using one of the following codes: **R** = Report, **P** = Prototype, **D** = Demonstrator, **O** = Other

[2] Please indicate the dissemination level using one of the following codes: **PU** = Public, **PP** = Restricted to other programme participants (incl. the Commission Services), **RE** = Restricted to a group specified by the consortium (incl. the Commission Services), **CO** = Confidential, only for members of the consortium (incl. the Commission Services)

Spatially-explicit midpoint and endpoint indicators on a global scale for terrestrial acidification

Authors (including participating authors not in involved in the LC-IMPACT project): Ligia B. Azevedo[1], Anna Kounina[2*], Pierre-Olivier Roy[3], Rosalie van Zelm[1], A. Jan Hendriks[1], Roland Bobbink[4], Louise Deschênes[3], Manuele Margni[2,3], and Mark Huijbregts[1]
*Corresponding author: Anna Kounina; e-mail: anna.kounina@quantis-intl.com
[1]Department of Environmental Science, Institute for Water and Wetland Research, Radboud University Nijmegen, P.O. Box 9010, 6500 GL, Nijmegen, The Netherlands
[2]QUANTIS, Parc scientifique de l'EPFL, Bât. D 1015 Lausanne Switzerland
[3]CIRAIG, École Polytechnique de Montréal (QC), P.O. Box 6079, stn centre-ville, Montreal H3C 3A7, Canada
[4]B-WARE Research Centre, Radboud University Nijmegen, P.O. Box 6558, 6503 GB Nijmegen, The Netherlands

Table of contents

Executive summary

A spatially-explicit global scale methodology for terrestrial acidification in Life Cycle Impact Assessment (LCIA) is currently unavailable. The objective of this work is to derive characterisation factors (CFs) that mathematically quantify the relation between an acidifying emission and its impact to the soil and to biodiversity. For this purpose, a characterization model has been developed that evaluates respectively the atmospheric fate, the soil sensitivity through changes in the hydrogen ion (H^+) concentration of soil solution, as well as through estimation of soil critical load and the effects in the form of the potentially not occurring fraction (PNOF) of vascular plant species.

The ILCD handbook (European Commission-Joint Research Centre - Institute for Environment and Sustainability, 2011) recommends to use the method of Accumulated Exceedance (AE) (Seppälä et al., 2006) updated by Pösch et al. (2008) at the midpoint level for the acidification impact category. It is, however, classified as "'recommended with some improvements needed' (Level II out of III)" (European Commission-Joint Research Centre - Institute for Environment and Sustainability, 2011). At the endpoint level, no method is recommended to be used because no methods are sufficiently mature to be recommended. However, van Zelm and colleagues' (2007) method is recommended as interim to be used for internal application (European Commission-Joint Research Centre - Institute for Environment and Sustainability, 2011).

In this project, LC-IMPACT, we develop two midpoint approaches (based on critical load and on H^+) and one endpoint approach based on the potentially not occurring fraction (PNOF) of species. The two methods are described in this deliverable. The comparison between the current and recommended midpoint and endpoint methods is shown in Tables 0.1 and 0.2.

At the midpoint level, we provide country (and continent) CFs worldwide; up to now, only CFs for European countries (and a general European continent CF) were available (Posch et al. 2008). We explore two midpoint methods in this work, both based on an atmospheric pollutant transport model across continents. To date, such models have not been used to calculate CFs. These two methods include soil sensitivity modeling based on (1) a geochemical soil model and (2) a critical load exceedance calculation. The spatial resolution, nonetheless, decreases to 2.0° x 2.5° degrees.

At the endpoint level, similar to the midpoint method, country and continent CFs are developed. Previously, country CFs were available only on a continental scale, e.g., for European countries for van Zelm et al.'s method (2007). Further, while the van Zelm et al. (2007) method covers generic European forest vegetation, the effect modeling developed during this project differentiates between vegetation types (biomes). In Europe, for example, forest types can vary from boreal forests in Scandinavia to mediterranean woodlands in Greece.

For a comprehensive assessment of the impact of acidification on terrestrial ecosystems, the authors of this report recommend that LCA's terrestrial acidification CFs include an evaluation of atmospheric fate and a soil sensitivity midpoint CF. A species sensitivity endpoint CF is also recommended, although there is a high uncertainty regarding endpoint modeling. The main limitation of the critical load method is that it cannot be used in combination with an effect factor. The critical load method thus cannot express the impact of acidification on ecosystems, and the impact score cannot be compared with other impact categories (e.g., eutrophication, ecotoxicity).

Table 0.1. Comparison of existing and recommended midpoint terrestrial acidification methods.

Midpoint	Recommended method (by this study)	Existing method (Posch et al. 2008)
Scale	Globe	Europe
Resolution	2.0° x 2.5°	0.5° x 0.5°[3]
Site-specificity	Yes	Yes
Atmopsheric transport across continents	Included	Not included
Nitrogen oxides ($NO_{x)}$	Included	Included
Ammonia (NH_3)	Included	Included
Sulfur dioxide (SO_2)	Included	Included
Spatial aggregation of CF	Country; Continent (all)	Country;[4] Continent (Europe only)
Emissions	Based on 2005 reports	Based on 2010 estimates

Table 0.2. Comparison of existing and recommended endpoint terrestrial acidification methods.

Endpoint	Recommended method (by this study)	Existing method (van Zelm et al. 2007)
Scale	Globe	Europe
Resolution	2.0° x 2.5°	50 km x 50 km
Site-specificity	Yes	Yes[5]
Atmopsheric transport across continents	Included	Not included
NO_x	Included	Included
NH_3	Included	Included
SO_2	Included	Included
Spatial aggregation of CF	Country; Continent (all)	Continent (Europe only)
Emissions	Based on 2005 reports	Based on 1990 to 2000 reports and 2001 to 2010 estimates

[3] Roughly 50 km x 50 km in European latitudes
[4] Only European countries
[5] Not specific for European forest types

1. Introduction

Project scope

Life Cycle Impact Assessment (LCIA) quantifies the environmental impact associated with the manufacture of a product or provision of a service (de Haes et al., 1999). LCIA can be performed at the midpoint or at the endpoint level. At the midpoint level, indicators measure the physicochemical processes occurring in the environment due to consumption of a resource or emission of a substance. Endpoint-level indicators describe the overall effects of these processes through societal values, such as ecosystem quality, human health and resource depletion. For the acidification impact category, midpoint indicators measure impact on environment along the cause-effect chain, such as changes in soil chemical properties, while at the endpoint, the indicator describes impact on the ecosystem, such as biodiversity losses (Roy et al., 2012a). An important advantage of endpoint LCIA is that the endpoint indicator can easily be compared in terms of unit across different impact categories, e.g. with the potentially not occurring fraction (PNOF) of species or potentially affected fraction (PAF) of species. In addition, endpoint indicators are easier to interpret and to be communicated for LCA practitioners given that all midpoint impact indicators are grouped in a reduced number of areas of protection, i.e., four categories for IMPACT 2002+ (Jolliet et al., 2003) which are understandable for non LCA experts (ecosystem quality, human health and resource depletion and global warming). On the other hand, endpoint LCIA introduces model uncertainties that are not present in a midpoint LCIA (Bare, 2010).

In order to translate the environmental impact of a given flow (e.g., emission) to or from the biosphere, LCIA employs characterisation factors (CFs). In the case of terrestrial acidification (or any other impact following the emission of a pollutant), the CF is the relationship between the emission of a substance and the impact on the environment. The acidification of terrestrial systems is mainly caused by nitrogen oxides (NO_x), ammonia (NH_3), and sulphur oxides (SO_2 and SO_4) (Roy et al., 2012a). Other acidifying pollutants include hydrogen chloride (HCl), hydrofluoric acid (HF), hydrogen sulfide (H_2S), and phosphoric acid (H_3PO_4), but given their short transport range (van Zelm et al., 2007), they are not taken into account in this study.

Contribution of this work to state-of-the-art LCIA methodologies

The main contributions of this work to current LCIA methodology for terrestrial acidification are as follows:

1- *Inclusion of atmospheric pollutant transport estimates across continents*: Current LCIA spatially-explicit methodologies for terrestrial acidification have been developed for specific countries or continents (Bare et al., 2003; Goedkoop and Spriensma, 2000; Hayashi et al., 2004; Huijbregts et al., 2000; Potting et al., 1998; Seppälä et al., 2006; van Zelm et al., 2007), although the transport of pollutants across continents has been shown to be relevant (Kajino et al., 2011). This work introduces the atmospheric transport of pollutants overseas following Roy et al. (Roy et al., 2012b).

2- *Inclusion of a critical load (CL) exceedance methodology for non-European areas*: Current LCIA CL exceedance frameworks include only emissions released in Europe and affecting the European continent (Posch et al., 2001; Seppälä et al., 2006). As emissions elsewhere have

become increasingly important (Kuylenstierna et al., 2001), this work introduces a framework for CL exceedances worldwide based on the method of Bouwman et al. (2002).

3- *Inclusion of a spatially-differentiated effect model to characterize the impact of soil acidification on plant diversity*: Current endpoint CFs for terrestrial acidification include a European-generic effect model based on European forest species (van Zelm et al., 2007) or a single plant species (Hayashi et al., 2004). This work introduces spatially-differentiated effect models based on the work of Azevedo et al. (2013), who showed that vegetation types respond differently to soil acidity (i.e., pH).

Environmental mechanism

The far majority of atmospheric emissions of acidifying pollutants occur following fossil fuel combustion or volatilization of urea fertilizer in agricultural fields (Bouwman et al., 2002). After atmospheric transformation, these pollutants are deposited on soils via dry or wet deposition and, consequently, change the chemical composition of the soil solution by increasing the concentration of hydrogen (H^+) and aluminum ions and reducing the cation exchange capacity and base saturation of soils (Bouwman et al., 2002). Ultimately, soils which undergo acidification may become unsuitable for survival of certain plant species (Falkengren-Grerup, 1986; Falkengren-Grerup et al., 1998).

2. Materials and Methods

Use of CFs in LCIA

LCIA computes CFs through the characterisation model framework proposed by De Haes et al. (2002). Emission data (E, expressing emitted mass of SO_2, NO_x and NH_3 in kg pollutant emitted·yr^{-1}) in generic landscape, continent, country or gridcell *i* for pollutant *p* from the inventory (LCI) are converted into impact category scores S by application of the CFs as presented in Equation 1.

$$S_{i,p} = \sum_p (E_{i,p} \cdot CF_{i,p}) \quad (1)$$

In order to generate impact scores over all locations, one can either calculate an average or a weighted average for location *i* by using weighting factor W to reflect unequal location size or importance, as follows:

$$S_{i,p} = \sum_i W_i \sum_p (E_{i,p} \cdot CF_{i,p}) \quad (2)$$

In the case that inventory data are available only at the country, continental or generic scale, the aggregated CF at the same scale should be applied.

Midpoint and endpoint CFs should be applied whenever possible, in order to analyse and compare results at both levels.

Characterisation models

The three characterisation models proposed by this study (Types 1 to 3) and their underlying fate and effect models are described in the following paragraph. This is followed by a description of how normalization scores can be obtained by combining pollutant emission estimates with the CFs derived in this work.

Characterisation factors Types 1 and 3 follow the framework of the current interim endpoint method (van Zelm et al., 2007), where a marginal change in an emission of pollutant *p*

from location *i* causes a change to soil properties of receiving location *j* and, ultimately, biodiversity of plants in *j*. Type 2 follows the framework of CL exceedance in a receiving compartment introduced by Bouwman et al. (2002).

Midpoint: Type 1

Type 1 CFs (mol $H^+ \cdot L^{-1} \cdot m^2 \cdot kg_{emitted}^{-1} \cdot yr$) for emitting location *i* for pollutant *p* are described following the work of Roy et al. (Unpublished) as:

$$CF_{i,p} = \sum_j (FF_{i,j,p} \cdot SF_{j,p}) \quad (3)$$

where $FF_{i,j,p}$ ($keq_{deposited} \cdot kg_{emitted}^{-1}$) describes the atmospheric fate factor of *p* (i.e., NO_x, NH_3, or SO_x) emitted from location *i* and deposited in location *j*; $SF_{j,p}$ (mol $H^+ \cdot L^{-1} \cdot m^2 \cdot keq_{deposited}^{-1} \cdot yr$) is the soil sensitivity factor of location *j* for deposited pollutant *p*.

Midpoint: Type 2

Type 2 CFs (meq $H^+ \cdot kg_{emitted}^{-1}$) for emitting location *i* for pollutant p are described following the work of Bouwman et al. (2002) as:

$$CF_{i,p} = \sum_j (FF_{i,j,p} \cdot t_{meq\_p} \cdot ER_j) \quad (4)$$

where t_{meq_p} (meq $H^+ \cdot kg^{-1}$) is a conversion factor from mass of pollutant *p* (kg) to miliequivalent of H^+ (meq H^+) and ER_j (dimensionless) is the critical load exceedance ratio for soil j.

Endpoint: Type 3

Type 3 CFs ($m^2 \cdot kg_{emitted}^{-1} \cdot yr$) for emitting location *i* for pollutant *p* are described following the work of Roy et al. (Unpublished) as:

$$CF_{i,p} = \sum_j (FF_{i,j,p} \cdot SF_{j,p} \cdot EF_j) \quad (5)$$

where EF_j (mol $H^{+-1} \cdot L$) is the effect factor in location *j*.

Fate and effect models

Atmospheric fate model

The atmospheric fate factor $FF_{i,j,p}$ is the increase in the deposition of pollutant *p* in *j* ($\Delta Dep_{j,p}$) following an increase in emission of *p* from *i* ($\Delta Em_{i,p}$). It is described following the work of Roy et al. (2012b) as

$$FF_{i,j,p} = \frac{\Delta Dep_{j,p}}{\Delta Em_{i,p}} \quad (6)$$

where $\Delta Dep_{j,p}$ ($keq_{deposited} \cdot yr^{-1}$) is the change in deposition of *p* on receiving soil *j* following a 10% increase in emission $\Delta Em_{i,p}$ ($kg_{emitted} \cdot yr^{-1}$) of *p* in *i*. This percentage increase is commonly used as a marginal increase in LCIA studies (Huijbregts et al., 2000; Krewitt et al., 2001; Potting et al., 1998). The $FF_{i,j,p}$ were obtained from Roy et al. (2012b), who calculated worldwide source receptor matrices (SRMs) resulting in spatially explicit atmospheric fate factors on a 2^{o}x2.5^{o} scale. For a given emission vector, the resulting grid-specific depositions are obtained by matrix-vector multiplication, avoiding the evaluation of the entire numerical (generally) non-linear model(s) of atmospheric transport and dispersion processes (Seibert and Frank, 2003).

Roy et al. (2012b) based their calculations on the GEOS-Chem global tropospheric chemistry model (Bey et al., 2001). GEOS-Chem is a 3D model of tropospheric chemistry driven by assimilated meteorological observations from the Goddard Earth Observing System (GEOS) of the NASA Data Assimilation Office (Bey et al., 2001). Roy et al. (Roy et al., 2012b) used the yearly averaged results from a GEOS-Chem 2^{o}x2.5^{o} grid spatial resolution simulation for the 2005 reference year, i.e. 2005 being representative of meteorology of the average from 1961 to 1990, according to the National Oceanic and Atmospheric Administration's National Climatic Data Center (2005).

Soil sensitivity model

The soil sensitivity factor $SF_{j,p}$ is the marginal increase in the concentration of H^+ (dC_j) following a marginal increase in the deposition of pollutant *p* in soil *j* ($dDep_{j,p}$). It is described following the work of Roy et al. (2012a) as:

$$SF_{j,p} = \frac{dC_j}{dDep_{j,p}} \cdot A_j = \frac{\Delta C_j}{\Delta Dep_{j,p}} \cdot A_j \quad (7)$$

where C_j (mol $H^+ \cdot L^{-1}$) is the H^+ concentration of soil solution of *j* in the receptor grid cell and A_j (m^2) is the area of *j*. In this study, A_j was defined by the sum of the areas of soils with the same PROFILE (See following paragraph for details) input parameters within a 2^{o}x2.5^{o} atmospheric grid. In total, 99515 receiving areas across the 13104 atmospheric grids were considered.

The soil sensitivity factors (SFs) were calculated with the PROFILE (Warfvinge and Sverdrup, 1992) geochemical steady-state model. PROFILE is based on a mass balance calculation for different soil layers. Among other outputs, it estimates the pH in the soil layer solution. The model requires atmospheric deposition values, weather characteristics and soil parameters (Supporting information 1). Following the ISRIC-Wise database (v 1.1) (Batjes, 2006), the soil depth was set to 1 m and split into five layers of 20 cm each. With this depth, we covered most (92 to 100%) of the vegetation root zone (Supporting information 1). To determine the SFs, averaged pH values were calculated using the biome-specific root distribution fraction from Jackson et al. (1996) as a weighting factor (Supporting information 1). We used the terrestrial ecoregion and biome classification (14 in total) by Olson et al. (2001).

Critical Load Exceedance Ratio

The model recommend in the ILCD handbook (European Commission-Joint Research Centre - Institute for Environment and Sustainability, 2011) developed successively by Seppälä et al. (2006)

and Posch et al. (2008) relies on the CL data generated for Europe in the context of the 1999 amendment of the 1979 Convention on Long-Range Transboundary Air Pollution (LRTAP) (Hettelingh et al., 2001). This CL data covers Europe and has not yet been developed on the global scale due to lack of availability of soil composition parameters. The only existing CL model applicable on a global scale is the one developed by Bouwman et al. (2002), relying on cation exchange capacity and base cations. The CL exceedance ratio ER_j is described following the work of Bouwman et al. (2002) as:

$$ER_j = \begin{cases} \mathrm{ER_j} = 0, \text{for } \dfrac{\mathrm{DepT2_j}}{\mathrm{CL_j}} \leq 1 & (8a) \\ \mathrm{ER_j} = \dfrac{\mathrm{DepT2_j}}{\mathrm{CL_j}}, \text{for } \dfrac{\mathrm{DepT2_j}}{\mathrm{CL_j}} > 1 & (8b) \end{cases}$$

where $\mathrm{CL_j}$ is the critical load (CL, $keq_{deposited} \cdot m^{-2} \cdot yr^{-1}$) threshold for soil *j*, and $\mathrm{DepT2}$ is the Type 2 total deposition acidifying pollutants into grid *j*. Harmful effects to soil occur when the sum of deposited charges $\mathrm{DepT2_j}$ ($keq_{deposited} \cdot m^{-2} \cdot yr^{-1}$) is greater than the CL for *j* (Eq. 6a). We assumed that emissions cause no harmful effects to soil if the total deposited charges do not exceed the CL (Eq. 6a) or if soils are covered by ice, rock and sea and, thus, $\mathrm{ER_j} = 0$. The calculations for$\mathrm{CL_j}$,$\mathrm{DepT2_j}$, and grid-specific $\mathrm{ER_j}$ are detailed in Supporting information 2.

Vegetation effect model

The effect factor EF_j is the marginal increase in the PNOF of vascular plant species ($dPNOF_j$, mol $H^{+-1} \cdot L$) following a marginal increase in the concentration of H^+ in *j* (dC_j). For example, an effect factor equal to 0.5 mol $H^{+-1} \cdot L$ indicates that the increase in 1.0 mol of H^+ triggers the potential non-appearance of 50% of vascular plant species in grid *j*. It is described following the work of Roy et al. (Unpublished) as:

$$EF_j = \frac{dPNOF_j}{dC_j} = -\left(PNOF_j\right)^2 \cdot \left[e^{-\frac{\left(log_{10}C_j + \alpha_j\right)}{\beta_j}}\right] \cdot \left[\frac{-1}{\beta_j} \cdot \frac{1}{C_j \cdot log_e 10}\right] \quad (9)$$

where α and β (dimensionless) are grid-specific coefficients illustrating respectively the concentration of H^+ at which the PNOF equals 0.5 and the slope of the function of PNOF and H^+. PNOF is described as a function of pH by Azevedo et al. (2013) for individual terrestrial biomes of the world. We used the map delineated by Olson et al. (2001) to recognize the biome type (14 in total) in each grid *j*. Biome-specific coefficients for the logistic curve of PNOF – pH (and, thus, PNOF – H^+) are described in Supporting information 3.

Uncertainty analysis

The influence of the FFs, SFs and EFs parameter uncertainty(ies) on the CFs uncertainty was evaluated with a Monte Carlo simulation (with random sampling, not latin hypercube).

Due to the complexity of the underlying atmospheric modeling input datasets interactions,

we considered FF a single parameter which varied at increasing intervals as the distance from the emission location increased. The variation of each FF was specified with a lognormal distribution. This distribution is defined by a geometric mean (calculated based on the arithmetic mean of generated FFs) and a standard deviation (calculated based on accuracy observations by Roy et al. (2012b), i.e., 25% accuracy at the emission location and up to 1000% accuracy at locations farthest from the emission location).

The SF uncertainty related to the accuracy of the input parameter was evaluated by Roy et al. (2012a). Consequently, each SF was considered to be lognormally distributed with an uncertainty factor of 100 (95% confidence interval).

The uncertainty of each EF was based on the uncertainty of the pH estimates (the working point of the pH – PNOF relationship curve) and the model regression α and β uncertainty. The 95% confidence intervals for pH were taken from Roy et al. (2012a). For α and β, the 95% confidence intervals were taken from Azevedo et al. (2013), as explained in Supporting information 3. For the biomes with model parameters derived from other biomes with similar climate conditions, we quantified an EF standard deviation originating from a switch from known parameters to parameters from a completely different "similar climate condition" biome (e.g. boreal forests parameters were approximated using mixed forests parameters instead). The uncertainty in the EFs for these two biomes was modelled with a lognormal distribution, defined by the calculated EFs and the standard deviation of pH values.

We then sampled 1000 values of FFs, SFs and EFs based on the specified uncertainty distributions. To ensure coherence, the sum of the sampled FFs related to one source location was evaluated and could not amount to more than 1 $kg_{deposited} \cdot kg_{emitted}^{-1}$. If the sum exceeded this limit, the samples were discarded and new values were sampled. With those samples we calculated 1 000 ∑FF, ∑FF·SF and CFs for each emitting grid, indicating the uncertainty in the grid-specific CF values.

Characterisation factors at larger spatial units

To derive CFs at larger spatial units *c* (i.e., country, continent, and world), we calculated the average of the CFs between emitting grids *i* located within the spatial unit *c* of interest based on their geographical coordinates (Supporting information 4).

Normalization factors

Non-weighted normalization factors

Grid-specific normalization factors (NF_i) are described as:

$$NF_i = \sum_p (CF_{i,p} \cdot E_{tot\,i,p}) \quad (10)$$

where $E_{tot\,i,p}$ ($kg_{emitted}^{-1} \cdot yr^{-1}$) is the total emission of pollutant *p* from emitting grid *i* in one year, based on 2005 emission data (2012b). The emissions $E_{tot\,i,p}$ for SO_2, SO_4, NO_x, nitric acid (HNO_3),

and NH_3 are given as kg of $SO_2 \cdot yr^{-1}$, kg of $SO_4 \cdot yr^{-1}$, and so on. For each of the three types of CFs (Types 1 to 3), the units for NF_i are mol $H^+ \cdot L^{-1} \cdot m^2$, meq H^+, and m^2, respectively. We employed emission data representative of the year 2005 following Roy et al. (2012b).

To derive NFs at larger spatial units *c* (i.e. country, continent, and world), we calculated the average of the NFs between emitting grids *i* located within the spatial unit *c* of interest based on their geographical coordinates (Supporting information 4).

3. Results

Characterisation factors

Types 1 and 3

Types 1 and 3 grid-specific CFs are shown in Figs. 1 and 2, respectively. Note that the numerical values of grid-specific CFs used in Figs. 1 and 2 are available in Supporting information 4. Type 1 CFs varied up to five orders of magnitude (Fig. 1), and the highest values were found in the Northern Hemisphere (particularly for acidifying pollutants based on NH_3 and SO_2).

High impacts to soil were attributed to emissions from Western China, Northern India, and Kazakhstan (Fig. 1a). Type 3 CFs also varied up to five orders of magnitude (Fig. 2). The largest Type 3 CFs were found for emission locations situated in central Asia, central Africa and Canada. CFs were largest for emission locations for which pollutants are then deposited on land characterized by large areas with low buffering capabilities (indicated by high pH change) and a working point of the pH-PNOF relationship curve associated with a steep slope value. The most frequent CF result for SO_2 (2.48 $m^2 \cdot yr \cdot kg_{emitted}^{-1}$) was higher than for NH_3 (2.43 $m^2 \cdot yr \cdot kg_{emitted}^{-1}$) and NO_x (1.33 $m^2 \cdot yr \cdot kg_{emitted}^{-1}$). For a given pollutant, CFs ranged over five (for NO_x and SO_2) to six (for NH_3) orders of magnitude. The spatial variability of the CFs of a given pollutant was several orders of magnitude higher than the variability between pollutants.

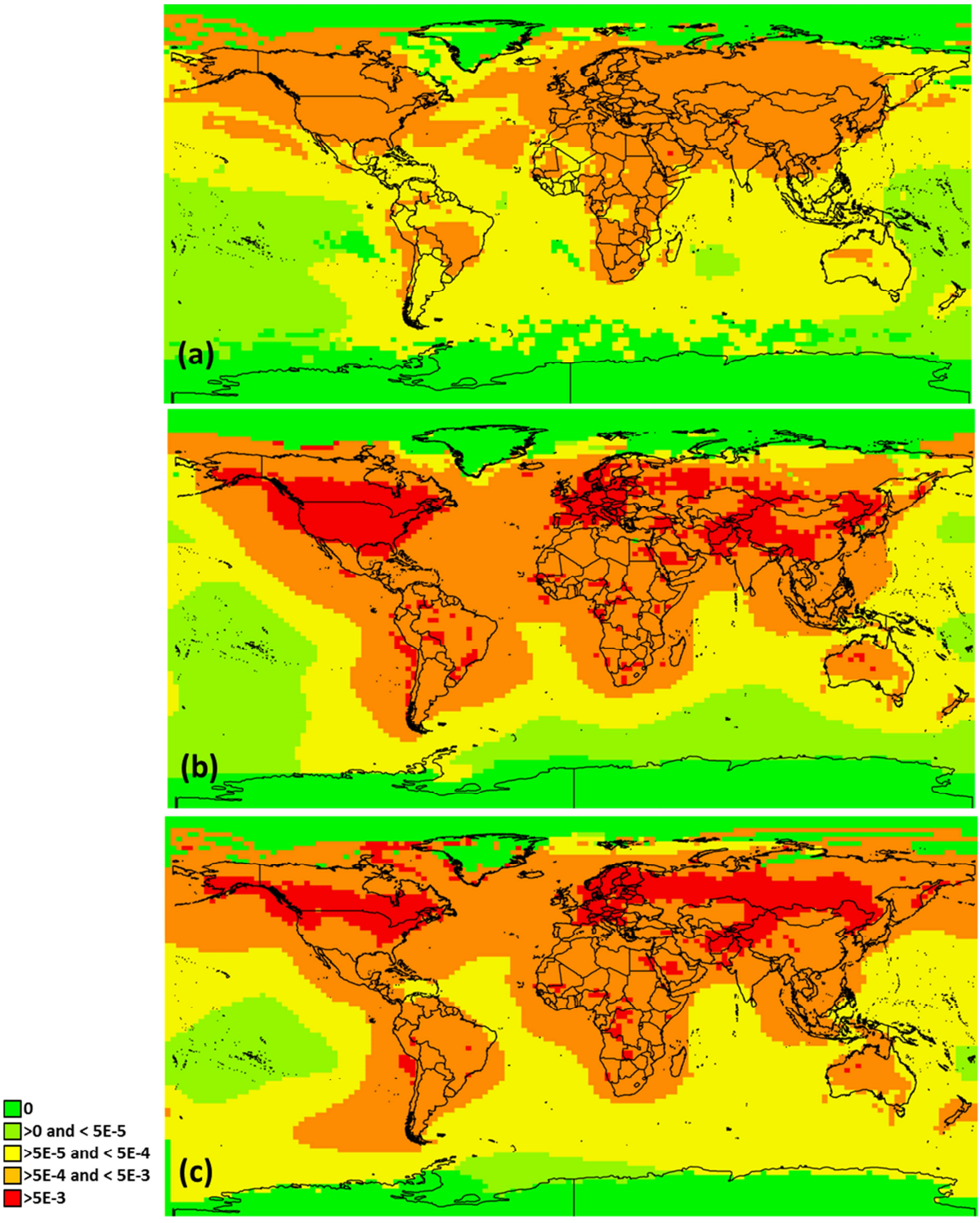

Fig. 1 Type 1 characterisation factors (mol $H^+ \cdot L^{-1} \cdot m^2 \cdot kg_{emitted}^{-1} \cdot yr$) for **(a)** NO_x, **(b)** NH_3, and **(c)** SO_2.

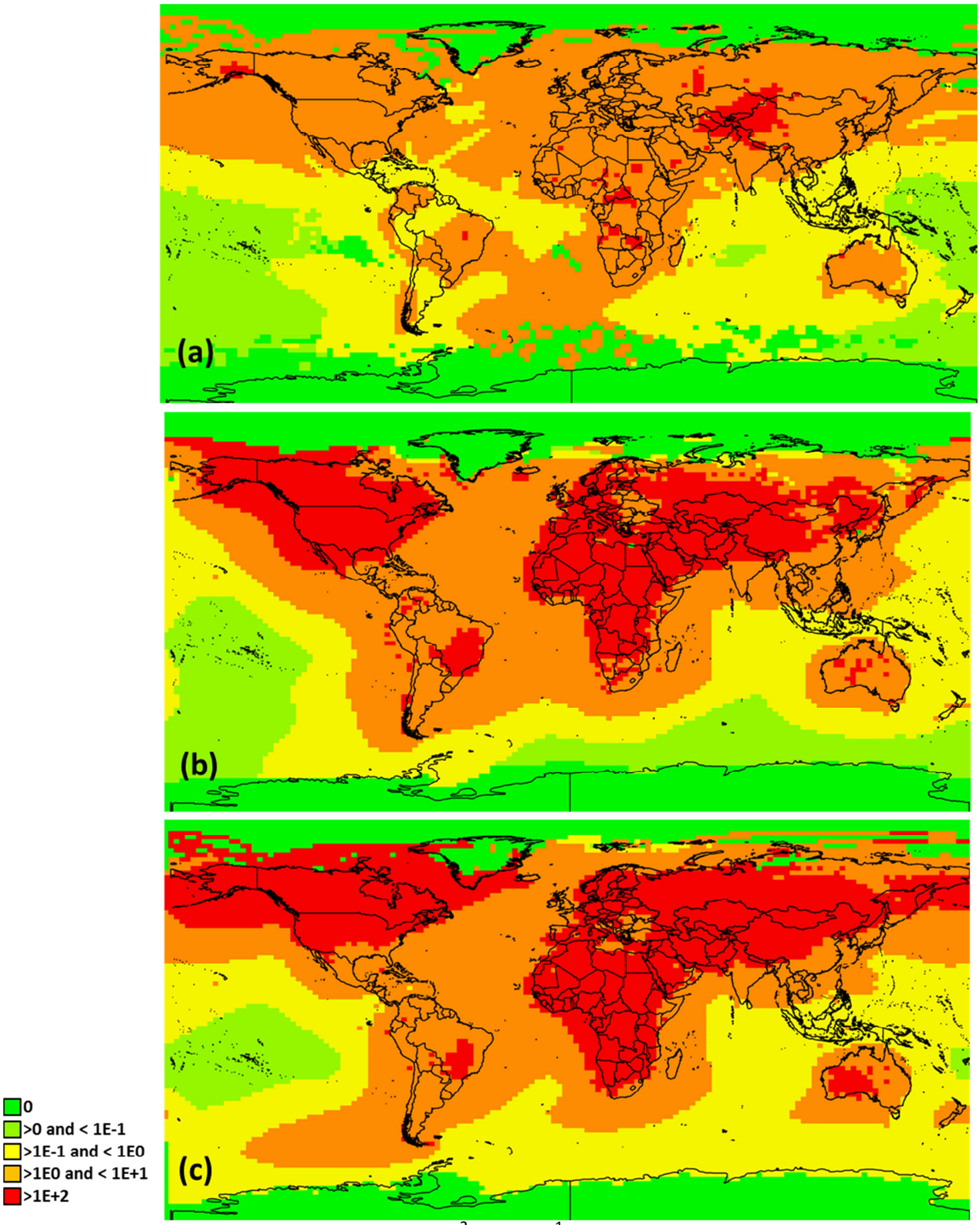

Fig. 2 Type 3 characterisation factors ($m^2 \cdot kg_{emitted}^{-1} \cdot yr$) for **(a)** NO_x, **(b)** NH_3, and **(c)** SO_2.

Type 2

Type 2 midpoint CF_i values followed the same distribution pattern for all three gases SO_2, NH_x and NO_x. Specifically, there were three main CL exceedance poles where the continental CF

exceeded 0.1 $meq_{deposited}$ $H^+ \cdot yr^{-1} \cdot kg_{emitted}^{-1} \cdot yr$: North America, Asia and Europe (Figure 6 (a),(b),(c)). Eastern Asia was the most affected area with values exceeding 15 $meq_{deposited} \cdot H^+ \cdot yr^{-1} \cdot kg_{emitted}^{-1} \cdot yr$ as a maximum. CL_j and ER_j used for CF_i calculation are mapped in Supporting information 1, and CF_i results on a continental and country scale are in Supporting information 4.

Countries with highest CF_i values are in $meq_{deposited}$ $H^+ \cdot yr^{-1} \cdot kg_{emitted}^{-1} \cdot yr$: Bangladesh with an average 2.3, Laos with 2.5, Netherlands with 2.3, Serbia with 2.4 and Vietnam with 2.2. These results reflected the fact that countries with large areas have heterogeneous results and cannot have an important country average CF_i. This lead to the conclusion that grid-scale analysis should be preferred to country-scale analysis given that the influence of the country area adds additional skew in the results.

A statistical analysis was performed to assess the variability of 2 x 2.5° CF_i results over continents. Figure 7 shows the lower quartile, median, upper quartile, the lowest datum still within 1.5 interquartile range (IQR) of the lower quartile, the highest datum still within 1.5 IQR of the upper quartile and the average in red. The average corresponds to the continental CF. From these figures and their detailed interpretation in Supporting information 6, we concluded that CF_is are heterogeneous in North America as well as in Asia, homogeneous with low values in South America, Africa and Oceania (CF_i<0.1 $meq_{deposited} \cdot H^+ \cdot yr^{-1} \cdot kg_{emitted}^{-1} \cdot yr$), and homogeneous with high values in Europe (CF_i>0.1 $meq_{deposited}$ $H^+ \cdot yr^{-1} \cdot kg_{emitted}^{-1} \cdot yr$). All gridcells were equal to zero for Antartica.

This statistical analysis confirmed that the continents with higher terrestrial acidification potential are Asia, Europe and North America, where average continental CF values are superior to 0.1. Other continents showed lower results by more than one order of magnitude and were not considered as overall significantly affected by exceedance of CL (using 2005 emission data and 2006 CL data). However, disparity of results in Asia as well as in North America showed that the use of continental scale CFs does not give sufficient accuracy in the CF_i range, and a gridcell scale analysis is thus preferred.

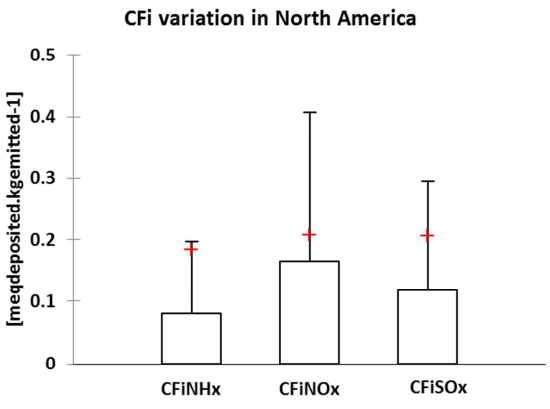

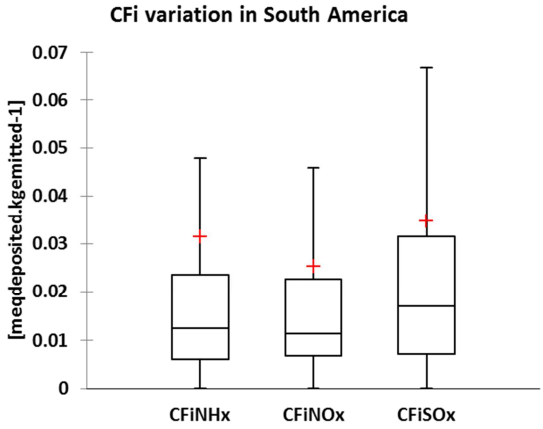

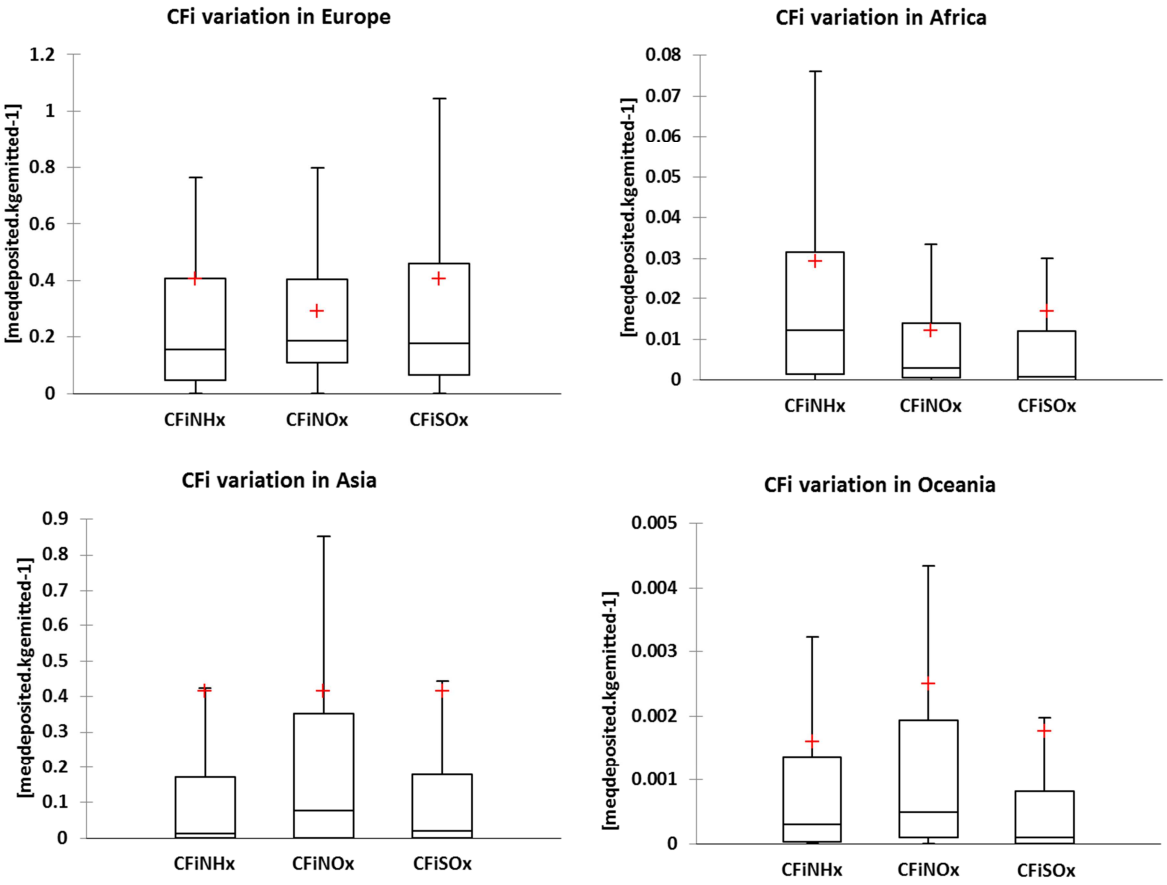

Fig. 3 Statistical analysis of spatially differentiated CF_i at 2°x2.5° grid within North America, South America, Europe, Africa, Asia and Oceania.

Comparison between spatial aggregation levels

The ratio between a 2^o x 2.5^o CF within a given spatial resolution and its coarser resolution CF was between 0.6-0.9, 1.1-1.7 and 1.0-1.3 for the global, continental and country resolutions, respectively (Fig. 4). This means that 2^o x 2.5^o CFs found within countries, for example, will be, on average, 1.0 to 1.3 times higher than the country CFs. It is also demonstrated that 24 to 36%, 4 to 12% and 1 to 4% of the 2^ox2.5^o CFs within the global, continental and country spatial resolutions, respectively, varied by more than one order of magnitude (Fig. 2, -1> ^{10}log (ratio) <1) as compared to the specified coarser spatial resolution CFs.

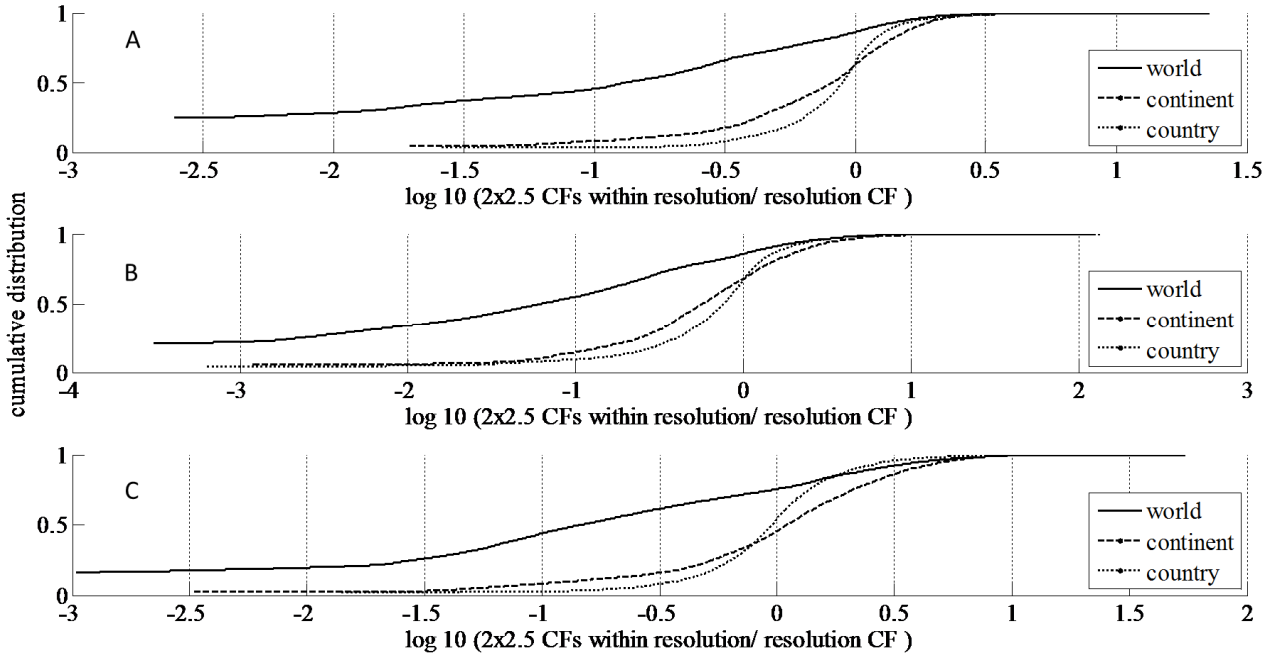

Fig. 4 Cumulative distribution of the $\log_{10}$ of the ratio between the 2^{o}x2.5^{o} CFs and the global, continental and country level resolution Type 3 CFs they fall in (x-axis) for emissions of **a)** NO_x, **b)** NH_3 and **c)** SO_2.

Uncertainty analysis

Results showed a variance of less than 0.06 for CF with different values of FF (∑FF) (Table 1). The variance CF for different values of FF and SF (∑FF×SF) is between 0.88 and 0.94 with slopes of the linear regression that are approximately 1. The strong correlation between ∑FF×SF and endpoint CFs was also confirmed by the relatively low standard error and residual sum of squares (RSS) of the regressions.

The ratios between the Monte Carlo varied and original ∑FF, ∑FF×SF and CF were found inside a $10^{\pm0.1}$ (0.79-1.26), $10^{\pm0.5}$ (0.32-3.2) and $10^{\pm1.5}$ (0.032-32) interval, respectively (Fig. 4). It was thus assumed that the FF is responsible for approximately 4%, SF for 6% and EF for 90% of the CFs' total evaluated uncertainty.

Table 1. Regression analysis of the spatial variability between endpoint characterisation factors (i.e., ∑FF×SF×EF) with both atmospheric fate (∑FF) and atmospheric fate-soil sensitivity (∑FF·SF) per emitted pollutants. R^2, σ, and RSS stand for coefficient of variation, standard deviation, and residual sum of squares.

	Equation of linear regression	R^2	σ	RSS
	∑FF and CF (i.e. ∑FF·SF·EF)			
NO_x	log (CF) = 0.4 log (∑FF) + 3.7	0.01	0.70	4748
NH_3	log (CF) = -2.0 log (∑FF) - 15.1	0.05	0.92	8798
SO_2	log (CF) = 0.9 log (∑FF) + 7.8	0.01	0.81	7124

	∑FF·SF and CF (i.e. ∑FF·SF·EF)			
NO_x	log (CF) = 1.0 log(∑FF×SF) + 3.8	0.94	0.17	287
NH_3	log (CF) = 1.0 log (∑FF×SF) + 3.6	0.95	0.22	499
SO_2	log (CF) = 1.1 log (∑FF×SF) + 3.9	0.90	0.26	744

4. Discussion

This study determined spatially-explicit CFs for terrestrial acidification at the global scale, thus enabling assessment of life cycle emissions occurring across the world. The following paragraphs (1) describe the main features and limitations of the Types 1 and 3 characterisation models, (2) compare results of this study to those of other studies, (3) discuss the outcome of EFs on the uncertainty of the characterisation model, and (4) recommend which midpoint and endpoint characterizatiom models should be used for terrestrial acidification LCIA.

Interpretation of results

Results showed that emissions in North America, Africa, western and northern Europe and central Asia generate high potential impacts, since high CFs values were observed in these areas. Roy et al. (2012b) showed that atmospheric FFs are highest at close proximity from the emission location. Roy et al. (2012a) showed that high SFs (resulting from a substantial change in H^+ concentration due to small deposits over a large area) occur in the Canadian shield region, the Scandinavian region, the Amazon basin, central Africa and parts of east and southeast Asia. Consequently, if assessment is limited to atmospheric fate and sensitivity, emissions in these locations will generate the highest impacts (i.e., high CFs).

However, due to the relatively high EF of “desert and xeric shrubland biome”, the regions of western North America (Nevada region), North Africa, central Asia and Western Australia also experience nontrivial impact. In biomes characterized by inherently low soil pH , e.g. (sub)tropical moist broadleaf forests, the EF was typically close to zero since the modeled pH was far from the pH zone where the steepest slope of the PNOF-pH regression occurs. Concurrently, as no weighting was performed based on the number of species in a biome or on the vegetation density, the method presented here represents the fraction (not the total number) of non-occurring species in an area. As a result, locations with a poor number of species will exhibit a higher affected fraction than very species-rich locations.

Limitations

This section discusses the limitations related to the assumptions and/or choices in the CF calculations. First, deposition was considered evenly distributed within a 2^{o}x2.5^{o} grid, neglecting local factors favoring deposition (e.g., mountains) within the grid. Global atmospheric models with greater resolution are required in order to account for these factors.

Second, terrestrial acidification can cause a number of other environmental impacts, including nutrient depletion, increased in soil solution H+ concentration (or decrease of pH), and increased concentrations of toxic aluminum species (Jeffries and Ouimet, 2004). By using soil solution H^+ concentration as the soil sensitivity indicator, the direct harm to the vegetation was

evaluated. The increase in soil solution H^+ concentration was chosen over the other types of indicators because it is recognized as a successful predictor of species richness and a primary indicator of soil acidity (Peppler-Lisbach and Kleyer, 2009; Whittaker, 1972). Furthermore, Roy et al. (Roy et al., 2012a) showed that other soil sensitivity indicators, such as aluminum concentration or nutrient concentration (in the form of base cations), are more sensitive to soil input parameters uncertainties as compared to soil solution pH.

Third, the assessment of a marginal change in emissions and deposition is still under discussion. Several authors (Huijbregts et al., 2000; Krewitt et al., 2001; Potting et al., 1998) used a +10% variation, while others tried a combination of different values with a maximum of 50% (Seppälä et al., 2006; van Zelm et al., 2007). These studies showed that results were insensitive to important incremental changes. Similarly, Roy et al. (2012a) tested the variation of the receiving environment's SF over 100 randomly chosen receiving environments with increments of depositions of 1%, 5% and 10%. The results indicated that a 1% change was not sufficient to create a change in pH values in numerous soils, while a quasi-linear relation between the registered pH at 5% and 10% increment was observed. Thus, we deemed a 10% increment to be acceptable.

Fourth, Azevedo et al. (2013) empirically identified an optimum pH--the pH at which species richness is highest. Accordingly, this study could have considered that there would be no effect at pH higher than the optimum, instead of extrapolating Azevedo et al. (2013) regression model to pH values higher than this optimum pH. However, if the optimum pH had been considered, only 33% of the soil areas would have EFs greater than zero (0). Furthermore, for some biomes, important gaps of non-occurring species near the optimum pH would have been registered. Such gaps could be observed with the desert and xeric shrubland biome, whichwould show a PNOF of 0 at pH = 7.4 but a PNOF of 0.14 following an infinitesimal decrease of pH. Extrapolation of the regression does not allow for a smooth transition over the entire pH range, a transition believed by the authors to be representative of natural processes. Nevertheless, the variation in CFs was quantified between both scenarios, and it was found that in 90% of the cases, CFs would be higher by less than 30% if we extended the regression model to the entire pH range, instead of considering an optimum pH (Supporting information 3).

Finally, unavailable model regression parameters impaired the effect assessment in Central America, India and the mountain regions of Asia. Indeed, these territories were approximated with parameters from other environments. The lack of data for these regions hinders accurate interpretation of the potential impacts.

Comparison to other studies

The European CFs developed in this study are compared with the CFs of Goedkoop and Spriensma (2000) and van Zelm et al. (2007); See Table 2. This study and van Zelm et al. (2007)'s results showed a similar relative importance of NO_x, NH_3 and SO_2 per unit emission. However, van Zelm et al. (2007) derived systematically lower CFs values. This may be explained by the fact that van Zelm et al. 1) used the EUTREND (Van Jaarsveld J. A. et al., 1997) atmospheric model, which does not include impacts caused by air emissions that travel outside of Europe; 2) used the dynamic soil model SMART (Kros et al., 1995), with which the steady-state simulation showed a 25 to 65% difference when using PROFILE to calculate CLs (Kurz et al., 1995); 3) assessed changes in soil base saturation instead of H+ concentration; 4) used a base saturation-PNOF dose-response

curve that yielded a gentler slope than the H+ concentration-PNOF dose-response, thus creating lower EFs in Europe; and/or 5) limited their assessment of potential impacts to European forest ecosystems, unlike the present assessment, which included numerous types of ecosystems.

The study of Goedkoop and Spriensma (2000) resulted in similar absolute CFs for NO_x and NH_3. However, the results differed significantly in terms of SO_2. This may be explained by the fact that Goedkoop and Spriensma (2000) (1) modeled impacts in the context of the Netherlands and then extrapolated their resulting EFs to Europe; (2) did not rely on atmospheric fate modelling, preferring a 10-mole marginal change to mapped deposition levels; (3) used the SMART model to evaluate changes in many soil properties, assessing the potential impacts of both acidification and eutrophication (SO_2 is not a eutrophying substance) instead of soil acidity changes, and (4) assessed the potentially disappeared fraction of species (PDF) for more than 900 Dutch plant species with the MOVE model (Latour and Reiling, 1993).

Table 2. Comparison of available biodiversity losses endpoint CFs and contribution of substances to the endpoint CF.

	Present study		**van Zelm et al. (2007)**		**Goedkoop and Spriensma (2000)**	
	CFs ($m^2 \cdot yr \cdot kg^{-1}$)	Contribution (%)	CFs ($m^2 \cdot yr \cdot kg^{-1}$)	Contribution (%)	CFs ($m^2 \cdot yr \cdot kg^{-1}$)	Contribution (%)
NO_x	5.9	12.5	0.4	15.6	5.7	25.6
NH_3	23.7	50.8	1.5	62.9	15.6	69.7
SO_2	17.1	36.6	0.5	21.5	1.0	4.66

Uncertainty analysis

Considering both spatial variability and uncertainty analysis results, the evaluation of both atmospheric fate and soil sensitivity could be seen as a trade-off between environmental relevance and uncertainty. While it is undeniable that the integration of ecological EFs in calculating endpoint CFs reveals information on the actual damage to ecosystems and allows for the meaningful aggregation of the consequences of different impacts, it can also be concluded that including the EF increases uncertainty typically without significant added value in terms of spatial variability.

Comparison between Type 1 and Type 2 CFs

Type 1 and Type 2 CFs relied on the same atmospheric FFs but differed in the exposure modeling. Although both models used the same database of soil properties (Batjes, 2009), the input parameters for the Type 2 CFs (i.e., cation exchange capacity and base saturation) are different than those for Type 1 CFs (i.e., change in H^+ concentration of soil solution). In addition, the changes in soil pH followed a 10% increase in emissions, while the CL exceedance model employed background emissions. Results on the gridcell and country level did not show correlation between Type 1 and Type 2 CFs due to these differences in exposure modelling.

Recommendations

Based on the outcomes of this study, it is recommended that calculation of terrestrial acidification CFs in LCA follows an integrated approach and includes an evaluation of (1) atmospheric fate and soil sensitivity with the Type 1 midpoint CF and (2) species sensitivity with Type 3 endpoint CF. This approach gives the opportunity to make a consistent midpoint and endpoint assessment by considering an EF, which is not possible with the CL method (Type 2 CF).

5. Conclusions

This work provides a consistent framework to derive spatially-explicit characterisation factors at both midpoint and endpoint levels at the global scale for terrestrial acidification. An atmospheric fate model (GEOS-Chem), a soil fate model (PROFILE), a CL model and a biome-specific vegetation effect model were implemented to achieve this. The GEOS-Chem model allowed for atmospheric pollutant transport across continents to be accounted. The PROFILE model, previously implemented in European studies, was extrapolated to all soils across the world. The CL model generated global results on a 5' by 5' resolution. The vegetation effect model was based on the framework of species-sensitivity distributions and was built on worldwide empirical data from literature. Midpoint and endpoint CFs were provided at country and continental scales. The high impact to soil occurs in high latitude areas of Canada, Scandinavia, and Eastern Russia due to the low acid neutralizing capacity (ANC) of these soils combined with the important SO_2, NH_3 and NO_X emissions in these areas. North America, Africa, Western and Northern Europe and central Asia exhibit the highest endpoint CFs. In these locations, impact to soil is enhanced by the presence of sensitive ecosystems, such as the boreal forests of Canada and Scandinavia, and/or the presence of highly pH-sensitive species.

This study found that atmospheric FFs show little spatial variability. Consequently, impact assessment based solely on atmospheric fate is not sufficient to differentiate between the potential impacts of the same product or service at different emission locations. The multiplication of the soil SF by the atmospheric FF demonstrated the importance of considering the sensitivity of soils to spatial variability. Also showed by this study, a low correlation exists between soil chemical indicators reaction modeling CFs (Type 1 CFs) and CL based CFs (Type 2 CFs). The difference between the models is related to exposure modeling, specifically soil sensitivity indicators, soil indicators change modelling, difference between marginal and background emissions modelling.

It is therefore recommended that computation of terrestrial acidification CFs in LCA follows an integrated approach and includes an evaluation of atmospheric fate and soil sensitivity with Type 1 midpoint CFs as well as an evaluation of species sensitivity with Type 3 endpoint CFs.

REFERENCES

Aherne, J., Sverdrup, H., Farrell, E.P., Cummins, T., 1998. Application of the SAFE model to a Norway spruce stand at Ballyhooly, Ireland. Forest Ecology and Management 101, 331-338.
Alveteg, M., Walse, C., Sverdrup, H., 1998. Evaluating simplifications used in regional applications of the SAFE and MAKEDEP models. Ecological Modelling 107, 265-277.
Azevedo, L.B., van Zelm, R., Hendriks, A.J., Bobbink, R., Huijbregts, M.A.J., 2013. Global assessment of the effects of terrestrial acidification on plant species richness. Environmental Pollution 174, 10-15.
Bare, J., Norris, G., Pennington, D., McKone, T., 2003. TRACI: The tool for the reduction and assessment of chemical and other environmental impacts. Journal of Industrial Ecolology 6, 49–78.
Bare, J.C., 2010. Life cycle impact assessment research developments and needs. Clean Technologies and Environmental Policy 12, 341-351.
Batjes, N.H., 2006. ISRIC-Wise derived soil properties on a 5 by 5 arc-minutes global grid (version 1.1); Report 2006/02, ISRIC-World Soil Information, Wageningen (with data set). p 55.
Batjes, N.H., 2009. Harmonized soil profile data for applications at global and continental scales: updates to the WISE database. Soil Use and Management 25, 124-127.
Bey, I., Jacob, D., Yantosca, R., Logan, J., Field, B., Fiore, A., Li, Q., Liu, H., Mickley, L., Schultz, M., 2001. Global modeling of tropospheric chemistry with assimilated meteorology: Model description and evaluation. Journal of Geophysical research 106, 23073-23905.
Bouwman, A.F., Fung, I., Matthews, E., John, J., 1993. Global analysis of the potential for N2O production in natural soils. Global Biogeochemical Cycles 7, 557-597.
Bouwman, A.F., Van Vuuren, D.P., Derwent, R.G., Posch, M., 2002. A global analysis of acidification and eutrophication of terrestrial ecosystems. Water Air and Soil Pollution 141, 349-382.
Butler, T.M., Lawrence, M.G., Gurjar, B.R., Aardenne, J.v., Schultz, M., Lelieveld, J., 2008. Evaluation of EDGAR data in representing emissions from megacities: the representation of emissions from megacities in global emission inventories. Atmospheric Environment 42, 703-719.
de Haes, H., Jolliet, O., Finnveden, G., Hauschild, M., Krewitt, W., Müller-Wenk, R., 1999. Best available practice regarding impact categories and category indicators in life cycle impact assessment. The International Journal of Life Cycle Assessment 4, 66-74.
de Haes, U., Jolliet, O., Finnveden, G., Goedkoop, M., Hauschild, M., Hertwich, E., Hofstetter, P., Klöpffer, W., Krewitt, W., Lindeijer, E., Mueller-Wenk, R., Olson, S., Pennington, D., Potting, J., Steen, B., 2002. Life-cycle impact assessment: Striving towards best practice. SETAC.
Duan, L., Huang, Y.M., Hao, J.M., Xie, S.D., Hou, M., 2004. Vegetation uptake of nitrogen and base cations in China and its role in soil acidification. Science of The Total Environment 330, 187-198.
European Commission-Joint Research Centre - Institute for Environment and Sustainability, 2011. Recommendations for Life Cycle Impact Assessment in the European context EUR 24571 EN, Luxemburg.
Falkengren-Grerup, U., 1986. Soil acidification and vegetation changes in deciduous forest in Southern-Sweeden. Oecologia 70, 339-347.
Falkengren-Grerup, U., Brunet, J., Diekmann, M., 1998. Nitrogen mineralisation in deciduous forest soils in south Sweden in gradients of soil acidity and deposition. Environmental Pollution 102, 415-420.
Goedkoop, M., Spriensma, R., 2000. The Eco-indicator 99: A Damage Oriented Method for Life Cycle Assessment, Methodology Report, second edition, in: Consultants, P. (Ed.), Amersfoort, Netherlands.
Hayashi, K., Okazaki, M., Itsubo, N., Inaba, A., 2004. Development of damage function of acidification for terrestrial ecosystems based on the effect of aluminum toxicity on net primary production. The International Journal of Life Cycle Assessment 9, 13-22.
Hettelingh, J.P., Posch, M., De Smet, P.A.M., 2001. Multi-effect critical loads used in multi-pollutant reduction agreement in Europe. Water, Air, and Soil pollution 130, 1133-1138.
Hijmans, R.J., Cameron, S.E., Parra, J.L., Jones, P.G., Jarvis, A., 2005. Very high resolution interpolated climate surfaces for global land areas. International Journal of Climatology 25, 1965-1978.
Hodson, M.E., Langan, S.J., Wilson, M.J., 1996. A sensitivity analysis of the PROFILE model in relation to the calculation of soil weathering rates. Applied Geochemistry 11, 835-844.

Huijbregts, M.A.J., Schöpp, W., Verkuijlen, E., Heijungs, R., Reijnders, L., 2000. Spatially explicit characterization of acidifying and eutrophying air pollution in life cycle assessment. Journal of Industrial Ecology 4, 75-92.
Jackson, Canadell, Ehleringer, Mooney, Sala, Schulze, 1996. A global analysis of root distributions for terrestrial biomes. Oecologia 108, 389-411.
Jeffries, D.S., Ouimet, R., 2004. Évaluation scientifique 2004 des dépôts acides au Canada, in: Canada, E. (Ed.). Service Météorologique Canada, Downsview, p. 440.
Jolliet, O., Margni, M., Charles, R., Humbert, S., Payet, J., Rebitzer, G., Rosenbaum, R., 2003. IMPACT 2002+: A new life cycle impact assessment methodology. The International Journal of Life Cycle Assessment 8, 324-330.
Jönsson, C., Warfvinge, P., Sverdrup, H., 1995. Uncertainty in predicting weathering rate and environmental-stress factors with the PROFILE model. Water Air and Soil Pollution 81, 1-23.
Kajino, M., Ueda, H., Sato, K., Sakurai, T., 2011. Spatial distribution of the source-receptor relationship of sulfur in Northeast Asia. Atmospheric Chemistry and Physics 11, 6475-6491.
Kottek, M., Grieser, J., Beck, C., Rudolf, B., Rubel, F., 2006. World Map of the Köppen-Geiger climate classification updated. Meteorologische Zeitschrift 15, 259-263.
Krewitt, W., Trukenmuller, A., Bachmann, T.M., Heck, T., 2001. Country-specific damage factors for air pollutants - A step towards site dependent life cycle impact assessment. International Journal of Life Cycle Assessment 6, 199-210.
Kros, J., Reinds, G.J., De Vries, W., Latour, J.B., Bollen, M., 1995. Modelling the response of terrestrial ecosystems to acidification and desiccation scenarios. Water, Air, & Soil Pollution 85, 1101-1106.
Kurz, D., Eggenberger, U., Rihm, B., 1995. Evaluating critical loads of acidity for Swiss forest soils: Comparison of two calculation methods. Water, Air, Soil Pollution 85, 2533-2538.
Kuylenstierna, J.C.I., Rodhe, H., Cinderby, S., Hicks, K., 2001. Acidification in developing countries: Ecosystem sensitivity and the critical load approach on a global scale. Ambio 30, 20-28.
Latour, J.B., Reiling, R., 1993. A multiple stress model for vegetation ('move'): a tool for scenario studies and standard-setting. Science of The Total Environment 134, Supplement 2, 1513-1526.
NOAA National Climatic Data Center, 2005. State of the Climate: Global Analysis for Annual 2005.
NRCS, U., 2009. Natural Resources Conservation Service, Soil Survey Laboratory Soil Characterization Data Query Interface. In United States Departement of Agriculture.
Olson, D.M., Dinerstein, E., Wikramanayake, E.D., Burgess, N.D., Powell, G.V.N., Underwood, E.C., D'Amico, J.A., Itoua, I., Strand, H.E., Morrison, J.C., Loucks, C.J., Allnutt, T.F., Ricketts, T.H., Kura, Y., Lamoreux, J.F., Wettengel, W.W., Hedao, P., Kassem, K.R., 2001. Terrestrial ecoregions of the worlds: A new map of life on Earth. BioScience 51, 933-938.
Peppler-Lisbach, C., Kleyer, M., 2009. Patterns of species richness and turnover along the pH gradient in deciduous forests: testing the continuum hypothesis. Journal of Vegetation Science 20, 984-995.
Posch, M., Hettelingh, J.-P., De Smet, P.A.M., 2001. Characterization of critical load exceedances in Europe. Water Air and Soil Pollution 130, 1139-1144.
Posch, M., Seppälä, J., Hettelingh, J.P., Johansson, M., Margni, M., Jolliet, O., 2008. The role of atmospheric dispersion models and ecosystem sensitivity in the determination of characterisation factors for acidifying and eutrophying emissions in LCIA. Internation Journal of Life Cycle Assessment 13, 477–486.
Potting, J., Schöpp, W., Blok, K., Hauschild, M., 1998. Site-dependent life-cycle impact assessment of acidification. Journal of Industrial Ecology 2, 63-87.
Rawls, W.J., Brakensiek, D.L., Saxton, K.E., 1982. Estimation of soil-water properties. Transactions of the Asae 25, 1316-&.
Reich, P., Eswaran, H., 2005. Global Soil Regions Map. Natural Resources Conservation Service.
Reynolds, B., 1997. Predicting soil acidification trends at Plynlimon using the SAFE model. Hydrology and Earth System Sciences 1, 717-728.
Roy, P.-O., Azevedo, L.B., Margni, M., van Zelm, R., Deschênes, L., Huijbregts, M.A.J., Unpublished. Uncertainty and spatial variability in characterization factors for terrestrial acidification at the global scale.

Roy, P.-O., Deschênes, L., Margni, M., 2012a. Life Cycle Impact Assessment of Terrestrial Acidification:Modeling Spatially Explicit Soil Sensitivity at the Global Scale. Environmental Science & Technology 45, 8270–8278.
Roy, P.-O., Deschênes, L., Margni, M., Huijbregts, M.A.J., 2012b. Spatially-differentiated atmospheric source-receptor relationships for nitrogen oxides, sulfur oxides and ammonia emissions at the global scale for life cycle impact assessment. Atmospheric Environment.
Seibert, P., Frank, A., 2003. Source-receptor matrix calculation with a Langrangian particle dispersion model in backward mode. Atmospheric chemistry and Physics Discussions 3, 4515-4548.
Seppälä, J., Posch, M., Johansson, M., Hettelingh, J.-P., 2006. Country-dependent characterisation factors for acidification and terrestrial eutrophication based on accumulated exceedance as an impact category indicator. The International Journal of Life Cycle Assessment 11, 403-416.
Tegen, I., Fung, I., 1995. CONTRIBUTION TO THE ATMOSPHERIC MINERAL AEROSOL LOAD FROM LAND-SURFACE MODIFICATION. Journal of Geophysical Research-Atmospheres 100, 18707-18726.
Van Jaarsveld J. A., Van Pul W. A. J, M., D.L.F.A.A., 1997. Modelling transport and deposition of persistent organic pollutants in the European region Atmospheric Environment 31, 1011-1024.
van Zelm, R., Huijbregts, M.A.J., Van Jaarsveld, H.A., Reinds, G.J., De Zwart, D., Struijs, J., Van de Meent, D., 2007. Time horizon dependent characterization factors for acidification in life-cycle assessment based on forest plant species occurrence in Europe. Environmental Science & Technology 41, 922-927.
Warfvinge, P., Sverdrup, H., 1992. Calculating critical loads of acid deposition with PROFILE — A steady-state soil chemistry model. Water, Air, & Soil Pollution 63, 119-143.
Whittaker, R.H., 1972. Evolution and Measurement of Species Diversity. Taxon 21, 213-251.
Zobler, L., 1986. A world soil file for global modeling, NASA Tech. Memo. 87802.

A list of input parameters for the model PROFILE is shown in Table S1.1. The calculation of soil SFs based on PROFILE were described in detail by Roy et al. (2012a).

The multiple (soil) layer approach of the PROFILE model makes it possible to assess the indicator values based on root distribution across soil layers. Root distribution according to depth was estimated as:

$$RF_n = 1 - \omega^d \quad \text{(S1.1)}$$

where (RF_n) is the cumulative root fraction from the soil surface to depth d (cm) and ω is the fitted extinction coefficient. Known ω values and calculated root distribution as a function of terrestrial biomes are shown in Table S1.2.

The five-layer pH values (1 per soil layer n) were aggregated into a single value indicator using roots distribution as a weighting factor as:

$$pH_j = \sum_n (pH_n \cdot RF_n) \quad \text{(S1.2)}$$

Table S1.1 PROFILE parameter description.

Parameters	Description	Spatial resolution
	Weather parameters	
Precipitation [m]	WorldClim-Global climate database (Hijmans et al., 2005)	10 arc minutes
Temperature [^{o}C]	WorldClim-Global climate database (Hijmans et al., 2005)	10 arc minutes
	Atmospheric deposition [keq/ha/yr]	
Acidifying substances wet and dry deposition	Deposition from GEOS-Chem for 2005 (Bey et al., 2001)	2^{o}x 2.5^o
Chloride, sodium and magnesium deposition	Percentage of sea-salt deposition from GEOS-Chem for 2005 (Roy et al., 2012b)	2^{o}x 2.5^o
Calcium deposition	10% of soil dust deposition (Roy et al., 2012b)	4^{o}x 5^o
Potassium deposition	2% of soil dust depositon (Roy et al., 2012b)	4^{o}x 5^o
	Soil parameters	
Layer height [cm]	Set to follow the ISRIC-Wise database (Batjes, 2006)	5x5 arc minutes
Soil texture	ISRIC-Wise database (Batjes, 2006)	5x5 arc minutes

Parameters	Description	Spatial resolution
[% sand, silt, clay]		
Soil water content [m^3 water/m^3 soil]	Maximum water content is a function of soil texture. Water content was assumed to be 80% of field capacity (Rawls et al., 1982)	5x5 arc minutes
Soil bulk density [kg/m^3]	ISRIC-Wise database (Batjes, 2006)	5x5 arc minutes
Water entering/leaving layer (%)	ISRIC-Wise database FAO qualitative drainage class to which a value of *absorbed water percentage* was attributed (Aherne et al., 1998; Alveteg et al., 1998; Batjes, 2006; Hodson et al., 1996; Jönsson et al., 1995; Reynolds, 1997; Warfvinge and Sverdrup, 1992)	5x5 arc minutes
Surface area [m^2/m^3]	Calculated in PROFILE (Warfvinge and Sverdrup, 1992)	-
Runoff [m]	Calculated in PROFILE (Warfvinge and Sverdrup, 1992)	-
Net uptake [keq/ha/yr]	Worldwide vegetation types map (Olson et al., 2001) was used to determine net uptake values from Duan et al. (2004)	0.5^ox 0.5^o
Dissolved organic carbon (DOC) [mg/l]	Calculated from the total organic carbon (TOC), dry bulk density, water content and typical values of DOC from literature (Aherne et al., 1998; Alveteg et al., 1998; Batjes, 2006; Hodson et al., 1996; Jönsson et al., 1995; Reynolds, 1997; Warfvinge and Sverdrup, 1992)	5x5 arc minutes
Mineralogy [% minerals]	A global soil order classification map was used to determine an average mineralogy, which was obtained from sampling data (NRCS, 2009; Reich and Eswaran, 2005)	-
Al_{exp} [unitless]	Default value: 3 (Warfvinge and Sverdrup, 1992)	-
log K_{Al} [$kmol^2/m^3$]	Soil layer default values (Aherne et al., 1998; Alveteg et al., 1998; Batjes, 2006; Hodson et al., 1996; Jönsson et al., 1995; Reynolds, 1997; Warfvinge and Sverdrup, 1992)	-
Carbon dioxide (CO_2) pressure [atm]	Soil layer default values (Aherne et al., 1998; Alveteg et al., 1998; Batjes, 2006; Hodson et al., 1996; Jönsson et al., 1995; Reynolds, 1997; Warfvinge and Sverdrup, 1992)	-
BC/N uptake efficiency [unitless]	Soil layer default values (Aherne et al., 1998; Alveteg et al., 1998; Batjes, 2006; Hodson et al., 1996; Jönsson et al., 1995; Reynolds, 1997; Warfvinge and Sverdrup, 1992)	-
N-immobilisation and denitrification [keq/ha/yr]	Followed the method in Bouwman et al. (2002)	5x5 arc minutes

Table S1.2 ω and root distribution fractions according to terrestrial biomes.

		Fraction of roots by layers of 20 cm				
Biomes	ω	0-20 cm	20-40 cm	40-60 cm	60-80 cm	80-100 cm
Tundra	0.914	0.83	0.14	0.02	0.00	0.00
Boreal forest / Taiga	0.943	0.69	0.21	0.07	0.02	0.01
Temperate conifer forests	0.976	0.38	0.24	0.15	0.09	0.06
Temperate broadleaf and mixed forests	0.971	0.44	0.25	0.14	0.08	0.04
Montane grasslands and shrublands	-	0.2	0.2	0.2	0.2	0.2
Temperate grasslands, savannas and shrublands	0.943	0.69	0.21	0.07	0.02	0.01
Mediterranean forests, woodlands and scrub	0.966	0.50	0.25	0.13	0.06	0.03
Desert and xeric shrublands	0.975	0.40	0.24	0.14	0.09	0.05
(Sub)tropical moist broadleaf forest	0.961	0.55	0.25	0.11	0.05	0.02
(Sub)tropical grasslands, savannas and shrublands	0.972	0.43	0.25	0.14	0.08	0.04
(Sub)tropical coniferous forests	0.961	0.55	0.25	0.11	0.05	0.02
(Sub)tropical dry broadleaf forests	0.961	0.55	0.25	0.11	0.05	0.02
Flooded grasslands and savannas	-	0.2	0.2	0.2	0.2	0.2
Mangroves	-	0.2	0.2	0.2	0.2	0.2

SUPPORTING INFORMATION 2

The critical load CL_j in receiving grid *j*, which is dependent upon cation exchange capacity and base saturation was obtained following the classification proposed by Bouwman et al. (2002), Table S2.1.

Type 2 total deposition of acidifying pollutants on grid *j* $\mathrm{DepT2_j}$ (meq·m^{-2}·yr^{-1}) was calculated following Bouwman et al. (2002) as

$$\mathrm{DepT2_j} = \sum_p \sum_i \left[\left(FF_{i,j,p} \cdot ET2_{i,p} \cdot t_{meq\_p} \cdot A_j^{-1} - N_{p,j} \right) \cdot \left(1 - f_{p,j} \right) - x \cdot t_{meq\_BC} \cdot BC_j \cdot A_j^{-1} \right] \quad \text{(S2.1)}$$

where $FF_{i,j,p}$ is the atmospheric fate factor ($kg_{deposited} \cdot kg_{emitted}^{-1}$), $ET2_{i,p}$ ($kg_{emitted}$) is the Type 2 total emission of pollutant *p* from emitting grid *i* deposited into *j*, t_{meq_p} (meq·kg^{-1}) is a conversion factor from mass of pollutant *p* (kg) to miliequivalents (meq), A_j is the area (m^2) subjected to the atmospheric deposition the deposition, $N_{j,p}$ ($meq_N \cdot m^{-2}$) is the nitrogen immobilization rate, $f_{p,j}$ (dimensionless) is the fraction of nitrogen lost by denitrification, x (dimensionless) is an adjustment factor, t_{meq_BC} (=4159 meq·kg^{-1}) is a unit conversion factor for base cation deposition, BC_j (kg·m^{-2}·yr^{-1}) is the base cation deposition in grid *j*.

Emission estimates $ET2_{i,p}$ were obtained from the EDGAR database (Butler et al., 2008). t_{meq_p} for nitrogen and sulphur are, respectively, 71,393 and 31,185 meq·kg^{-1}. $N_{p,j}$ is given as:

$$N_{j,p} = \begin{cases} 0, for\ p = SO_x & \text{(S2.2a)} \\ N_i \cdot \dfrac{\sum_j FF_{i,j,NO_x}}{\sum_j FF_{i,j,NO_x} + \sum_j FF_{i,j,NH_3}}, for\ p = NO_x & \text{(S2.2b)} \\ N_i \cdot \dfrac{\sum_j FF_{i,j,NH_3}}{\sum_j FF_{i,j,NO_x} + \sum_j FF_{i,j,NH_3}}, for\ p = NH_3 & \text{(S2.2c)} \end{cases}$$

where N_i is the long term net immobilization rate (5.4 $meq_N \cdot m^{-2} \cdot yr^{-1}$) suggested by Bouwman et al. (2002).

$f_{p,j}$ was determined based on the drainage class of different soil taxonomic groups following Zobler et al. (1986) and Bouwman et al. (1993), Table S2.1. The $f_{p,j}$ for very poorly drained, poorly drained, imperfectly drained, well to moderately well drained, and excessively to well drained soils were given as 0.8, 0.6, 0.5, 0.4, and 0.2, respectively (Bouwman et al., 2002).

Table S2.1 $f_{p,j}$ depending on the drainage class of different soil taxonomic groups (Bouwman et al., 1993; Zobler, 1986).

Drainage class definitions	**1 = very poorly drained** **2 = poorly drained** **3 = imperfectly drained** **4 = well to moderately well drained**

	5 = excessively to well drained
Soil taxonomic group	**Drainage class**
acrisol	3
cambisol	1
chernozem	1
podzoluvisol	2
rendzina	1
ferralsol	1
gleysol	5
phaeozem	2
lithosol	1
fluvisol	1
kastanozem	1
luvisol	3
greyzem	3
nitosol	1
histosol	5
podzosol	2
arenosol	1
regosol	1
solonetz	3
andosol	1
ranker	1
vertisol	3
planosol	3
xerosol	1
yermosol	1
solonchek	1
ice	-

The adjustment factor x_p is given as:

$$x_p = \begin{cases} \frac{\sum_i FF_{i,j,p}}{\sum_p \sum_i FF_{i,j,p}} \cdot \frac{BC}{Dust} \end{cases} \quad \text{(S2.3)}$$

where $\frac{BC}{Dust}$ is the ratio of base cation to dust deposition, suggested by Tegen and Fung (1995) as equal to 0.2.

BC_j data were obtained based on the 4°×5° resolution map by Tegen and Fung (1995).

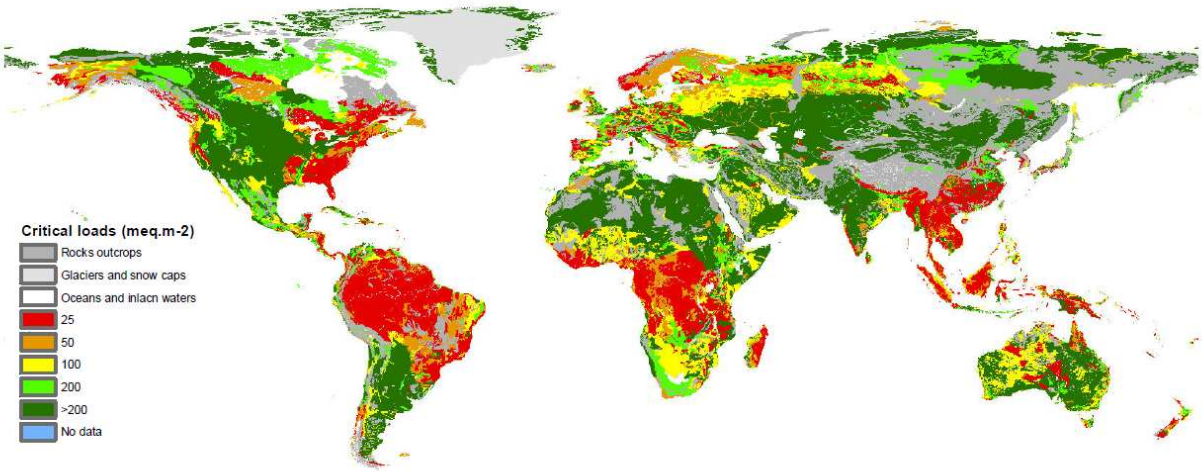

Figure S2.1 Critical load (CL) map on a 5'×5' resolution (Bouwman et al., 2002). The map was adapted to a 2° x 2.5° resolution grid for this study. Spatial recalculation of CL from a 5' x 5' to a 2° x 2.5° resolution was performed by using the most frequent value of CL in an array in order to prevent occurrence of positive CL values in coastal zones dominated by sea area.

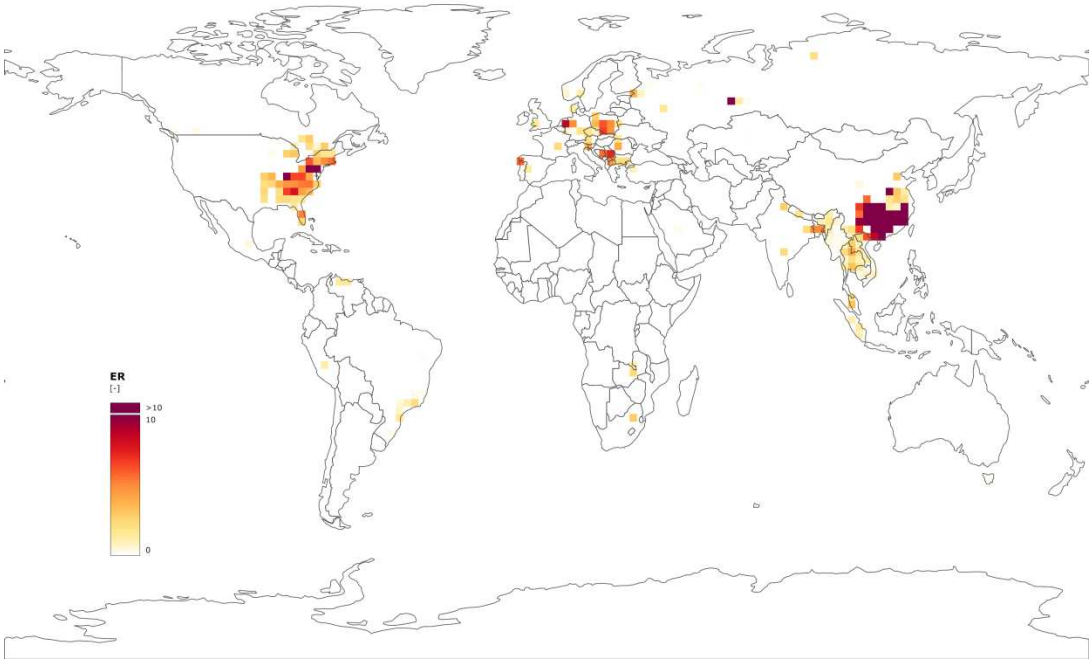

Fig. S2.2 Exceedance ratio (ER_j) on a 2°×2.5° resolution.

SUPPORTING INFORMATION 3

Biome-specific PNOF – pH logistic functions were derived for vascular plant species by Azevedo et al. (2013) as:

$$PNOF_{i,j} = \frac{1}{1+e^{-\left(\frac{\alpha_j - pH_j}{\beta_j}\right)}} = \frac{1}{1+e^{-\left(\frac{\alpha_j + log_{10}C_j}{\beta_j}\right)}} \quad \text{(S3.1)}$$

where pH_j is the soil pH (dimensionless), C_j is the concentration of H^+ (mol $H^+ \cdot L^{-1}$), and α_j and β_j are logistic-regression coefficients of grid *j* (Table S3.1).

The PNOF functions are based on observational field data where species occurrence at individual pH ranges is confirmed but factual absence is not. Accordingly, we chose PNOF as our impact indicator since we could not verify that the fraction of species disappeared. The latter is represented by the potentially disappeared fraction, PDF.

The coefficients α and β were not available for the (sub)tropical coniferous forest and (sub)tropical dry broadleaf forest biomes. Thus, for grids located in these biomes, we employed the coefficients derived originally for the (sub)tropical moist broadleaf forest biome based on the similarity of climates according to the Köppen-Geiger classification (Kottek et al., 2006).

Table S3.1 pH optimum and biome-specific coefficients α and β (95% confidence interval) for different terrestrial biomes of the world, source: Azevedo et al. (2013). NS stands for non-significant at the 95% confidence level.

Biome	(Range of) optimum pH	α	β
(Sub)Tropical Moist Broadleaf Forest	4.1	3.55 (3.51 to 3.6)	0.18 (0.14 to 0.22)
(Sub)tropical grassland, savanna, and shrubland	4.9	4.55 (4.40 to 4.70)	0.16 (NS)
(Sub)Tropical coniferous forest		Not available	
Mangrove	4.3 to 6.0	3.72 (3.67 to 3.77)	0.25 (0.20 to 0.30)
(Sub)tropical dry broadleaf forest	7	Not available	
Flooded grassland and savanna	5.9 to 6.6	5.31 (5.10 to 5.51)	0.33 (0.14 to 0.53)
Desert and xeric shrubland	7.4	6.76 (6.68 to 6.83)	0.36 (0.28 to 0.36)
Mediterranean Forest, Woodland, and Shrubland	7.8	6.64 (6.21 to 7.08)	1.18 (0.54 to 1.83)
Temperate Broadleaf Mixed Forest	4.7 to 5.1	3.57 (3.53 to 3.61)	0.36 (0.32 to 0.40)
Temperate Grassland, Savanna, and Shrubland	5.1 to 5.7	4.42 (4.37 to 4.47)	0.26 (0.22 to 0.31)
Temperate Coniferous	4.7 to 4.8	3.33 (3.17 to 3.50)	0.28 (0.11 to 0.44)

Forest			
Montane grassland and shrubland	6.0 to 7.0	5.92 (NS)	0.01 (NS)
Boreal Forest / Taiga	5.3	4.21 (4.09 to 4.32)	0.69 (0.55 to 0.84)
Tundra and alpine	7.0 to 7.3	4.76 (4.62 to 4.90)	0.47 (0.33 to 0.61)

SUPPORTING INFORMATION 4

This supporting information describes the Microsoft Excel spreadsheets accompanying this deliverable (Table S4.1).

Table S4.1 Description of accompanying Microsoft Excel spreadsheets.

Variable	Unit	Referenced in	Worksheets	Spreadsheet
Characterisation factor $CF_{i,p}$ (Type 1 and Type 3)	Type 1: mol $H^+ \cdot L^{-1} \cdot m^2 \cdot kg_{emitted}^{-1} \cdot$ yr Type 3: $m^2 \cdot kg_{emitted}^{-1} \cdot yr$	Eq. 1 and 3	'GridMidCF' 'CountryMidCF' 'ContinentMidCF' 'GlobalMidCF' 'GridEndCF' 'CountryEndCF' 'ContinentEndCF' 'GlobalEndCF'	'CF.xlsx'
Emission data $E_{i,p}$	kg of $SO_2 \cdot yr^{-1}$, kg of $SO_4 \cdot yr^{-1}$, kg of $NO_x \cdot yr^{-1}$, kg of $HNO_3 \cdot yr^{-1}$, and kg of $NH_3 \cdot yr^{-1}$	Eq. 8	'GridEmiss' 'CountryEmiss' 'ContinentEmiss' 'GlobalEmiss'	'Emissions.xlsx'
Non-weighted normalization score NF_i	Type 1: mol $H^+ \cdot L^{-1} \cdot m^2$ Type 3: m^2	Eq. 8 and 9	'GridMidNS' 'CountryMidNS' 'ContinentMidNS' 'GlobalMidNS' 'GridEndNS' 'CountryEndNS' 'ContinentEndNS' 'GlobalEndNS'	'NS.xlsx'